

## MODELING OF TRANSPORT PROCESSES IN THE CIGARETTE PRINCIPLE COMBUSTION FURNACE

by

**Aleksandar M. ERIĆ<sup>a,\*</sup>, Stevan Dj. NEMODA<sup>a</sup>, Mirko S. KOMATINA<sup>b</sup>,  
Branislav S. REPIĆ<sup>a</sup>, and Dragoljub V. DAKIĆ<sup>c</sup>**

<sup>a</sup>Vinca Institute of Nuclear Sciences, University of Belgrade, Belgrade, Serbia

<sup>b</sup>Faculty of Mechanical Engineering, University of Belgrade, Belgrade, Serbia

<sup>c</sup>Innovation Centre, Faculty of Mechanical Engineering, University of Belgrade,  
Belgrade, Serbia

Original scientific paper

<https://doi.org/10.2298/TSCI180226318E>

*This paper presents numerical and experimental investigations of complex and interrelated physical and chemical phenomena that occur during combustion of baled soybean residue in the furnace with the cigarette type of combustion. The result of comprehensive research is reactive flow model of biomass combustion inside furnace. Model is described by set of PDE which define momentum, heat and mass transfer processes in porous and fluid system. The main aim of developed CFD model is numerical simulation of combustion process inside the cigarette furnace. It is also used to provide deeper insight in complex processes occurring during biomass combustion.*

*Verification of proposed numerical model was performed through comprehensive experimental tests on the experimental-industrial plant of 1.5 MW boiler for heating the greenhouses in the Agricultural Corporation in Belgrade. The tests included measurement of flow rate and air and flue gas temperature input and output values on the furnace that are taken as the boundary conditions of the developed model. Comparison of the experimental results shows satisfactory agreement with numerical results (the maximum relative deviation of calculation and measurement temperatures are 10-45%), therefore the developed mathematical model could be used to analyse the effects of structural and parametric (fuel composition, power rate, air excess etc.) changes of the facility, from the standpoint of energy efficiency and ecology.*

Key words: baled biomass, combustion, modeling, experimental

### Introduction

The use of RES is becoming more and more important [1], mainly due to continuously increasing prices of fossil fuels, resources depletion and global attempts to achieve maximum feasible CO<sub>2</sub> emission reduction. Researches in this area are very complex and in order to obtain reliable data it is necessary to carry out theoretical and experimental research of the process. For this purpose, a 1.5 MW industrial-scale hot water boiler was constructed and installed in the Agricultural Corporation, Belgrade. The boiler is based on waste baled soybean residue combustion and it is used for heating 1 ha (10,000 m<sup>2</sup>) of greenhouses. Combustion in the boiler carried on so-called *cigarette* principle [1-3] where 0.7 × 1.2 × 2.0 m straw bales are used as fuel.

The scheme of the combustion chamber within the pilot plant is shown in fig. 1(a). Baled straw is fed to the furnace by the means of hydraulic cylinder system. After entering the

\*Corresponding author, e-mail: erica@vinca.rs

rectangular water-cooled feeding duct, bales are conveyed by a motor driven variable-speed driven controlled conveyor and directed towards the furnace. The primary combustion air is divided into two streams. Preheated primary air is injected into the furnace, more specifically into the area of the furnace surrounding the straw bale. In addition, a portion of the primary air is injected from bottom ash chamber, which is placed under the water-cooled grate. The ash fluidization is carried out by this part of the air-flow. Combustion of unburnt biomass completes within the fluidized ash area. Using a bottom ash screw conveyor to remove the ash is extracted from the system thus the desired height of fluidized bed has been retained. The secondary air is introduced through water-cooled secondary air inlet directly into the char combustion zone. This device has the possibility of alternating rotational movement around its axis, left-to-right. With rectilinear motion, along the axis, furnace power is regulated (allowing the smaller or larger amounts of biomass involved in the combustion process), and by rotational movement, around its axis, the ash is removed from top of the bale. Flue gases created in the primary combustion chamber after the turn entering the secondary and tertiary chamber where the gas completes combustion process then continue to the heat exchanger areas and the stack.

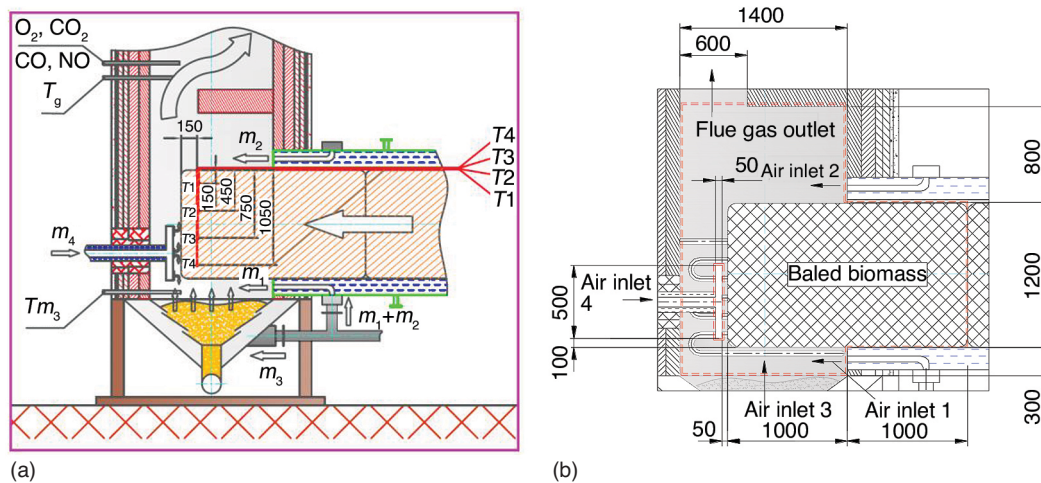


Figure 1. Experimental scheme; (a) scheme of measurement points, (b) model geometry

Since this is a relatively new and insufficient analysed technology, a complex CFD simulation of the combustion process by the proposed procedure may be important for future research. Numerical simulation of operation of such systems involves modeling the momentum, heat and substance transfer process of the combustion of baled biomass which have a porous media structure [4]. For developing a mathematical model of combustion parameters except thermophysical porous media properties [4-6], it is very important to know the input (boundary) values, and output parameters because of its verification.

### Mathematical model

Numerical simulation of the considered facility involves modeling of momentum, heat and mass transfer processes occurring during combustion of biomass bales, which have a porous media structure. It is therefore understood that combustion processes occurring in the boiler needed to be modeled both with respect to processes occurring in porous media (biomass bale) as well as processes occurring in the fluid media (the area in the furnace surrounding the biomass bale).

Based on the literature review of theoretical studies conducted [1, 2] and also taking into account the type of phenomena needed to be modelled, respective momentum, heat and mass transfer equations have been defined in order to accurately describe changes in the three primary parameters (velocity, concentration and temperature). Certain assumptions and simplifications have been adopted in order to eliminate the factors that were deemed to have very little effect on the processes analyzed and that would only contribute to the increased model complexity. The main assumption was that 2-D and stationary model, with constant position of the combustion front, was able to accurately describe the facility and processes analysed. The process is stationary, because the bale burns with the speed that is equivalent to the speed of incoming bale. Thus, porous layer *i.e.* the biomass fuel was assumed to be continuously fed into the combustion chamber, whereby all processes were considered stationary due to the fact that the biomass feed rate was equal to the rate of vaporization, devolatilization and char combustion. Fuel feeding process was simulated by volumetric sources of different fuel components present in the porous zone (moisture, volatiles and coke residue), defined based on the known boiler heat output. Porous medium was deemed homogeneous and characterized by uniform thermal and flow properties (porosity, permeability, thermal conductivity) across the porous layer. The specified thermal and flow properties were determined experimentally [5, 6]. The model assumed homogeneous combustion occurring both in the porous and the fluid medium, with Arrhenius equation utilized to describe the constant rate of chemical reactions. In addition, it was assumed that volatile components of the baled soybean residue comprised propane, CO<sub>2</sub>, and water vapour [4]. This approximation is carried out in such a way that all fuel products of devolatilization (CO, hydrogen, lower and higher hydrocarbons) are approximated with propane molecule and non-combustible with CO<sub>2</sub>. Energy conservation in the porous medium was modelled by solid-and-liquid-phase-temperature-balance model *i.e.* by one-equation, single-phase model.

The geometry of modelled area is presented in fig. 1(b). The model domain is defined by a dotted line. It can be seen that only one baled soybean residue has been taken into account due to numerical grid optimization, as well as computation time reduction. From fig. 1(b) we can see that the model consists of a porous (hatched area within the calculation domain) and fluid environment (shaded area within the calculation domain), with four input and one output cross-section. Transport processes are modelled assuming that the flow regime in both environments is turbulent, and turbulence is modelled using widespread and generally accepted *k-ε* model.

### Velocity field

The equation of continuity is the simplest transport equation in which the unsteady term has been omitted due to stationarity of the considered case. The velocity of the cross-section of porous layer substantially corresponds to the velocity in the fluid environment [4, 7, 8], so that it can be defined the momentum equation, which applies to the porous and the fluid environment in the following form:

$$\frac{\partial}{\partial x_i}(\rho_j W_j) = S_c \quad (1)$$

where  $S_c$  is the source which is defined by boundary conditions,  $i, j = 1, 2$  for 2-D case, and  $W_j$  is the velocity components ( $W_1$  i  $W_2$ ).

To define a velocity field it is also necessary to define the momentum equation, which is different for the fluid and porous media. The momentum equation for a fluid environment has its usual form, but the momentum equation porous media is different for an additional term due to of

pressure drop that occurs from fluid-flow through porous media. This pressure drop is usually defined by Forchheimer's equation that for higher velocities implies a non-linear dependence between fluid velocity and pressure gradient [4, 7, 8]. Based on this equation of momentum is defined in the following form:

$$\frac{\partial}{\partial x_i}(\rho_f W_i W_j) = \frac{\partial}{\partial x_i} \left( \mu_{\text{eff}} \frac{\partial W_j}{\partial x_i} \right) - \frac{\partial p}{\partial x_j} - \left( \frac{\mu_{\text{eff}}}{K_1} W_i + \frac{\rho_f}{K_2} W_i W_i \right) \quad (2)$$

where the turbulent stresses are determined by very widespread  $k$ - $\varepsilon$  model. For the purposes of the proposed model it was introduced the assumption that the turbulent viscosity coefficient in the porous area  $\mu_{e,p}$  is equal to the coefficient of turbulent viscosity in the free fluid zone  $\mu_k$ , so therefore their effective values are equal [4]. The coefficients  $K_1$  and  $K_2$  are Forchheimer's equation coefficients which are experimentally determined by [5, 6].

### Species concentration fields

The species concentration fields are defined by introducing the transport equations of chemical species, as well as in the case of momentum conservation equation for a fluid-flow, it has a common form with diffusion, convection and source term. Taking into account macroscopic examination of porous media as the fluid in which its influence on the species transport is considered through the effective diffusion coefficient, can be written the following relation:

$$\frac{\partial}{\partial x_i} (W_i \rho Y_k) = \frac{\partial}{\partial x_i} \left( \rho D_{\text{eff}} \frac{\partial Y_k}{\partial x_i} \right) + \varepsilon R_k \quad (3)$$

where  $D_{\text{eff}}$  is the effective diffusion coefficient. This coefficient, with neglecting of the turbulence range and value of dispersed turbulent diffusion, is defined:

$$D_{\text{eff}} = D_{\text{disp}} + \frac{1}{\rho} \left( \frac{\mu_\varepsilon}{\sigma_m} + \frac{\mu_{t\varepsilon}}{\sigma_t} \right) \quad (4)$$

where  $\sigma_m$  is Schmidt number of molecular diffusion, and  $D_{\text{disp}}$  is mass dispersion coefficient which according to de Lemos [8, 9] can be determined:

$$D_{\text{disp}} = \rho \frac{\mu_k}{\sigma_m} C \quad (5)$$

where  $C$  is the model constant which according to de Lemos [8, 9] for flow conditions in the considered model is approximately 100. However, because of calculations simplicity and macroscopic approaches of fluid-flow through porous media the dispersed mass diffusivity has been ignored and also has been adopted that  $\mu_{e,\varepsilon} = \mu$  and  $\mu_{t,\varepsilon} = \mu_t$ . Thus effective diffusion coefficient in the porous media becomes equal to the effective diffusion coefficient in the fluid-flow:

$$\frac{\partial}{\partial x_i} (W_i \rho Y_k) = \frac{\partial}{\partial x_i} \left[ \rho \left( D_{m,k} + \frac{\mu_t}{\rho \sigma_t} \right) \frac{\partial Y_k}{\partial x_i} \right] + \varepsilon R_k \quad (6)$$

The source term of this equation is multiplied by the porosity  $\varepsilon$ , because of assumption that the chemical reactions take place only within the porous cavity. The form of the source term,  $R_k$ , depends on the combustion process rate, as well as the stoichiometry of the process. Thus, the source term definition is based on these two parameters.

For the homogeneous reaction according [10] the modified Arrhenius's expression for the conversion components rates is often used:

$$R_k = M_k \sum_m^{i=1} (v_{\text{pik}} - v_{\text{rik}}) A_i T^{\alpha_i} \exp \left( -\frac{\Delta E_i}{R_g T} \right) \left( \prod c^{\nu_{\text{rik}}} \frac{1}{K_{c,i}} \prod c^{\nu_{\text{pik}}} \right) \quad (7)$$



where  $R_k$  is component  $k$  conversion rate,  $m$  – the number of chemical reactions,  $A_i$  – the preexponential coefficient for the reaction  $i$ ,  $a_i$  – the temperature coefficient,  $\Delta E$  – the activation energy for the reaction  $i$ ,  $v_{\text{pik}}$  and  $v_{\text{rik}}$  are stoichiometric numbers of products and reactants for the reaction  $i$  and component  $k$ , respectively. Where the following requirement has to be met:

$$\sum_{k=1}^m v_{\text{pik}} A_k = \sum_{k=1}^m v_{\text{rik}} A_k \quad (8)$$

where  $A_k$  is the atomic mass of the atomic species  $k$ . In this way the rates of combustion reactions, which are considered within the proposed model, have been defined.

For easy visibility the source terms of the chemical species conservation equations are shown in tab. 1.

For the purposes of the volatiles combustion modeling in accordance with the assumptions related on their composition, the two-stage reversible reaction of the propane combustion was adopted and accordingly the following model can be set, tab. 2:

**Table 1. Source term of the chemical species conservation equations**

| Species  | Source   |
|----------|--|
| $C_3H_8$ | $-R_{C,H_i}$   |
| CO       | $3 \frac{M_{CO}}{M_{C_3H_8}} R_{C_3H_8} - R_{CO} + \frac{M_{CO}}{M_{CO_2}} R_{CO_2} + \frac{M_{CO}}{M_C} R_C$  |
| $O_2$    | $-\frac{7}{2} \frac{M_{O_2}}{M_{C_3H_8}} R_{C_3H_8} - \frac{M_{O_2}}{M_{CO}} R_{CO} - \frac{1}{2} \frac{M_{O_2}}{M_C} R_C + \frac{1}{2} \frac{M_{O_2}}{M_{CO_2}} R_{CO_2}$ |
| $H_2O$   | $4 \frac{M_{H_2O}}{M_{C_3H_8}} R_{C_3H_8}$   |
| C        | $-R_C$   |
| $CO_2$   | $\frac{M_{CO_2}}{M_{CO}} R_{CO} - R_{CO_2}$  |

**Table 2. Conversion rates of components**

| Component | Reaction   | Conversion rate  |
|-----------|--|--|
| $C_3H_8$  | $C_3H_8 + \frac{7}{2} O_2 \rightarrow 3CO + 4H_2O$ | $R_{C,H_i} = \frac{d [C_3H_8]}{d\tau} = k_{o,1} e^{-\frac{E_1}{RT_x}} [C_3H_8]^{0.1} [O_2]^{1.65}$ |
| CO        | $CO + \frac{1}{2} O_2 \rightarrow CO_2$            | $R_{CO} = \frac{d [CO]}{d\tau} = k_{o,2} e^{-\frac{E_2}{RT_x}} [CO][O_2]^{0.25} [H_2O]^{0.5}$      |
| $C_2O$    | $CO_2 \rightarrow CO + \frac{1}{2} O_2$            | $R_{CO_2} = \frac{d [CO_2]}{d\tau} = k_{o,3} e^{-\frac{E_3}{RT_x}} [CO_2]$                         |
| C         | $C + \frac{1}{2} O_2 \rightarrow CO$               | $R_C = \frac{d [C]}{d\tau} = k_{o,4} e^{-\frac{E_4}{RT_x}} [C][O_2]$                               |

**Temperature fields**

In order to define this field in addition to the previously introduced equations it is necessary to introduce energy conservation equations for fluid and porous media.

In a similar way as in the case of species concentration fields the energy conservation equation in porous media has been defined. Here the porous media is also considering such a fluid flow where the influence of porous media parameters is reflected through the effective thermal conductivity (single phase model) [4]. Here is assumed that the effective diffusion coefficient of gases in porous media, responsible for transmitting the heat amount due to gases diffusion, has the same effective diffusion coefficient as in the fluid-flow. Hence, the expression of energy conservation equation for porous media can be defined:

$$\frac{\partial}{\partial x_i} (W_i \rho c_p T_f) = \frac{\partial}{\partial x_i} \left[ \frac{\lambda_{\text{eff}}}{c_p} \frac{\partial (c_p T_f)}{\partial x_i} \right] + e \sum R_k H_k + \frac{\partial}{\partial x_i} \left[ \sum \rho \left( D_{m,k} + \frac{\mu_t}{\rho \sigma_t} \right) (c_{p,k} T) \frac{\partial Y_k}{\partial x_i} \right] + q_r \quad (9)$$

The effective thermal conductivity of the fluid-flow through porous media is analyzed in detail in [4, 10, 11] where he highlighted the importance of two of its members: stagnant thermal conductivity and dispersed thermal conductivity. Similar to the diffusion coefficient in this case the modeling has been performed applying some simplification in terms of the impact of neglect the dispersed thermal conductivity influence, because at high temperatures the stagnant thermal conductivity is dominant, due to the thermophysical properties of gases. Thus the effective heat transfer coefficient is defined:

$$\lambda_{\text{eff}} = \lambda_f \varepsilon + \lambda_s (1 - \varepsilon) \quad (10)$$

where  $\lambda_s$  is the coefficient of thermal conductivity of the porous solid matrix layer, or in this case, soybean residue, whose value is determined by experimental research, which are more described in [6].

The last member in the energy conservation equation is the radiation energy transfer within the gas-flow which is defined by P1 model (which is part of FLUENT 6 CFD package) and for the purposes of this mathematical model will be shown in somewhat different form because of assumption that the range of the external radiation is zero:

$$q_r = - \frac{1}{3(a - \sigma_s) - C\sigma_s} \nabla G \quad (11)$$

where  $G$  is the incoming radiation in the final volume, and the additional transport equation has been developed for  $G$  determination. The additional transport equation has been processed together with other transport equations of the model:

$$\frac{\partial}{\partial x_i} \left( \Gamma \frac{\partial G}{\partial x_i} \right) = aG - 4an^2 \sigma T^4 \quad (12)$$

The emission coefficient,  $a$ , in the radiation energy eq. (12) is determined by the Weighted-Sum-of-Gray-Gases Model which is presented by the equation:

$$a = \frac{\ln(1 - \epsilon_r)}{s} \quad (13)$$

By presented equations the mathematical formulation defining of the proposed baled soybean residue combustion model for the observed furnace construction, has been completed.

The PDE comprising the mathematical model used for simulation the combustion of baled soybean residue are non-linear and mutually coupled. Numerical procedure of solving the equations has been performed by using the control volume method, including the collocated numerical grid for momentum equations, hybrid numerical scheme (the combination of upstream and central differencing) and SIMPLE algorithm for solving the equations. The iteration process stabilization is done by sub-relaxation technique. The calculation procedure and the numerical method are described in more details in [12].

For the first calculations of the said system of PDE of baled soybean residue combustion model, has been solved using the adapted version of the open finite-volume CFD-code FASTEST-2D, with own developed modules for modeling of flows with combustion in porous matrix as well in surrounding turbulent flow.

There is no doubt that development of original models and respective numerical codes represent the best way to obtain appropriate numerical solution for a particular engineering problem. The said approach is deemed to be the most reliable and with more possibilities for easy implementations of own physical processes models. However, the said approach the said is not *friendly using* and the entire process is long-lasting. On the other hand, commercial CFD codes have recently achieved such a high level of efficiency and accuracy that their use in the research activities worldwide has demonstrated that the ones can be successfully used for simulation of high complexity flows with chemical reactions. One of these complex flows is the subject of this paper, which basic task is a simulation of the combustion process in a porous medium, as well in the surrounding fluid. It is of course necessary for the user of such code to be provided with a possibility to *intervene* in the code, *i.e.* to adjust a general model to the particular problem in question. In the commercial software FLUENT, version 6.3.26, this could be easily achieved using the *user-defined functions*. The software also contains an integrated modulus for computation of porous media flows. Moreover, the software allows own codes implementation (by the *user-defined functions*) for fuel feeding simulation by volumetric sources of different fuel components present in the porous zone (moisture, volatiles and coke residue), what is very difficult to achieve by the own code based on FASTEST-2D. For the said reasons the specified commercial CFD software has been selected to be used for reacting flow simulation in the presented research.

### Comparison of results of model and experiment

Experimental investigations at an industrial-boiler are designed to provide the necessary parameters to verify the proposed combustion model, with particular reference to the global process kinetics. The determination of the global process kinetics implies the measurement of the rate and degree of fuel conversion for the given experimental conditions, as well as the composition and temperature of the flue gases at the output cross-section of the model.

For this purpose, the following input parameters were measured:

- air mass-flows at the entrances  $\dot{m}_1, \dot{m}_2, \dot{m}_3,$  and  $\dot{m}_4,$
- flue gas temperature on the exit of the fluidized bed of ash  $T_{m3},$
- fuel mass-flow (baled soybean residue  $\dot{m}_{fu}),$
- the flue gas temperature at the outlet cross-section of the modelled area  $T_g,$  and
- the dry flue gas composition on the outlet cross-section of the modelled area ( $\text{CO}_2, \text{O}_2, \text{CO}, \text{NO}.$ )

The scheme of measurement points is shown in fig. 1(a). Measurement of mass-flows of air at inlet cross-sections was measured indirectly through the measurement of the velocity in the channels by the Pitot-Prandtl probe. The dynamic and static pressure difference was read on the pressure transducer (ALNOR) device. These values were not changed in the stationary mode, so they were measured only once

The flue gas temperatures at the exit from the fluidized bed of its own ash  $T_{m3}$  and the temperature at the output cross-section  $T_g$  were measured continuously with  $K$ -type thermocouples, and their reading and acquisition was carried out by the KEITHLEY acquirer, whose extended measurement uncertainty is  $0.8\text{ }^\circ\text{C}$  at full measuring range. Assuming that the measurement thermoparassic uncertainty for which these measurements were performed at  $0.5\text{ }^\circ\text{C}$  at a full measuring range, the total measurement uncertainty is  $0.94\text{ }^\circ\text{C}$  at the full measuring range.

The feeding of the baled soybean residue is carried out using a hydraulic feeder, but quasi-continuously, so that in a cycle of one minute, a certain number of seconds the bale travels to the combustion chamber, and the remaining time stays for up to one minute. Therefore, the

relative position of the bale to the entry into the combustion chamber was recorded in relation and time to get.

The volume composition of dry flue gases at the output cross-section was measured continuous using three types of gas analyzers: Servomex 4900 C1; M&S Product Analyzetechnik CtmbH; Fuji Electric Sysmes co Ltd., and the results is given in the appropriate diagrams.

This set of experimental tests was performed in order to compare the global kinetics of the combustion process with the proposed model. In order to compare the temperature profile in the bale with the model, a special experiment was performed to determine the temperature profile during the stationary operating regime of the plant. The measurement was carried out in such a way that four thermoparators of *K*-type were placed linearly in the central plane of the bale at a distance of 150 mm from its forehead, according to the scheme of fig. 1(a) and together with the ball placed in the feeding system. During the movement of the bale towards the combustion chamber, thermocouples measured the temperature and their position was recorded at a certain time interval, thus obtaining a 2-D profile of the temperature formed in the bale during its path from entering the combustion chamber to the combustion zone. The experiments used thermocouples in a 3 mm metal coil (coax) with a length exceeding 2 m, which was estimated to be insufficient to damage the compensation lines due to high temperature.

During experiments, the temperature of the furnace is between 850-900 °C, which is the optimal temperature for combustion of the baled soybean residue, which is sufficiently high for total combustion but is still safe from the ash melting point. Although the stationary measurement regime lasted considerably longer, the results of an hour of an hour would be displayed, which is quite sufficient to make the necessary conclusions about the quality of combustion and dispersion with the proposed model.

Figure 2 presents the domain of the mathematical model developed, with boundary conditions shown in tab. 3.

Comparing the experiment results and the model is shown in figs. 3-5. From the diagrams it can be seen that the satisfactory agreement between results of experiments and the model has been achieved. Temperature of the baled soybean residue in central cross-section obtained by the proposed model is 7 K higher than the measured mean temperature, and also the calculated value of the NO concentration is 10 ppm higher than the mean measured value.

These diagrams show the comparison of model and the results of experiments at the border cross-sections without analysis of the characteristic values within the entire calculating domain. However, in this work the

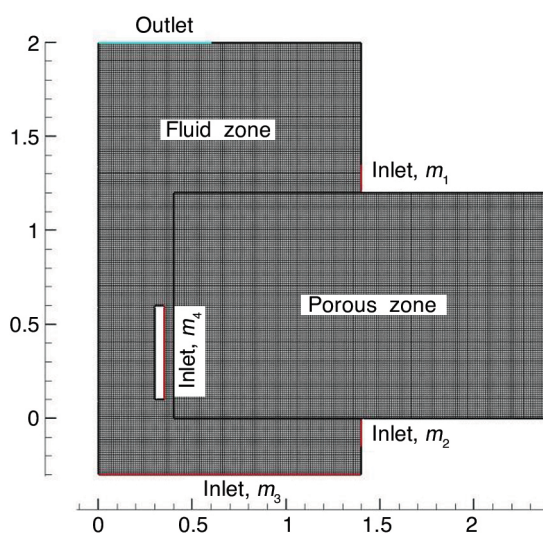


Figure 2. Numerical grid schemes and boundary conditions

Table 3. Boundary conditions on the front sections of the model

| Unit  | Mass-flow, [kgs <sup>-1</sup> ] |         |         |         | Mass-flow on fuel, [kgs <sup>-1</sup> ] |
|-------|---------------------------------|---------|---------|---------|---|
|       | Inlet 1                         | Inlet 2 | Inlet 3 | Inlet 4 |   |
| Value | 0.3486                          | 0.3843  | 0.3647  | 0.0455  | 0.112143                                |

comparison of the measured and modelled temperature field in the middle vertical plane of the bale has been carried out.

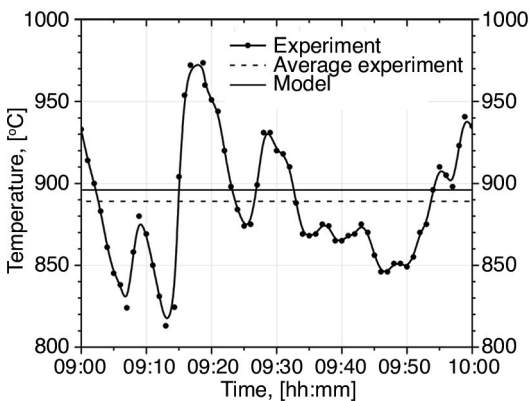


Figure 3. Flue gas temperature at the outlet cross-section

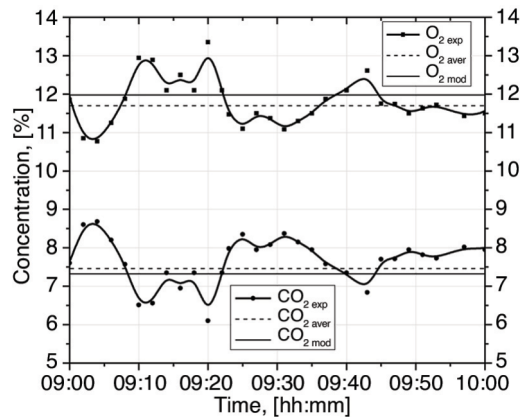


Figure 4. The O<sub>2</sub> and CO<sub>2</sub> concentrations in the flue gas at the outlet cross-section

Previous already has been pointed out that the feeding rate during the experiments was quasicontinuous so that the part of time bale moves toward to the combustion zone (work interval), and the remaining time (interval mode) the bale rests. From here it is clear that the mean speed of bale, if it is continuously moving, was less than the speed of movement in the work intervals. This statement is very important from the point of adopting relevant temperatures in the interval mode, because although it is generally a steady case, but there is unsteady heat conduction during the interval mode. If the movement of bales were uniformly and continuously, as adopted in the model defining, then the temperature for a period that corresponds to the interval mode probably has value in the interval between the maximum and minimum values of temperature measurements, but it is difficult to say with certainty whether the real temperature value was closer maximum, minimum or mean. Because of that the presentation of whole temperatures range has been adopted and its comparison with temperatures obtained by the proposed model, as it is shown in figs. 6-9. The calculated 1-D temperature profiles in figs. 6-9 are derived from the results of the 2-D numerical simulation. For the bale zero position has been adopted the end position of the combustion zone.

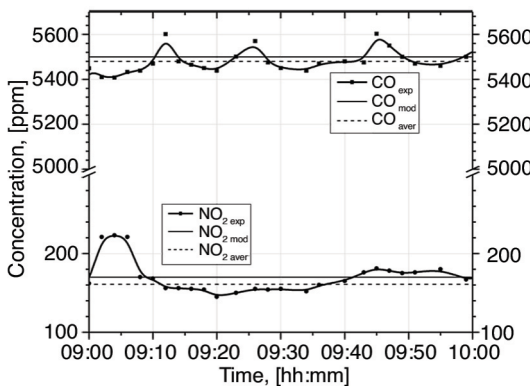


Figure 5. Concentrations of CO and NO in the combustion products at the outlet cross-section

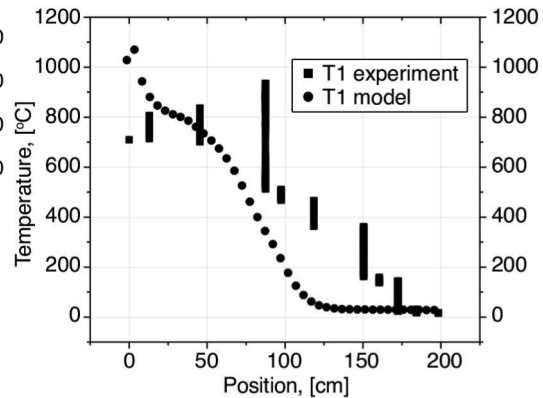


Figure 6. The temperature along the central cross-section of bale for the height  $y = 15$  cm



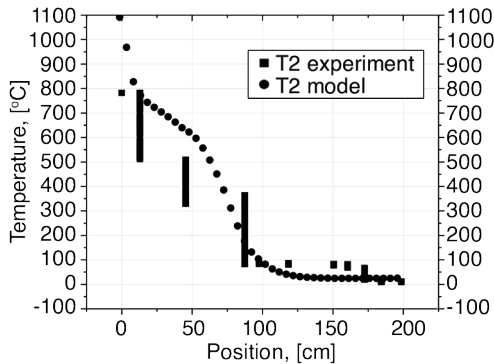


Figure 7. The temperature along the central cross-section of bale for the height  $y = 45$  cm

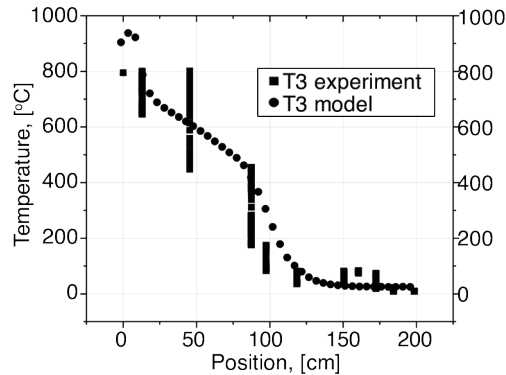


Figure 8. The temperature along the central cross-section of bale for the height  $y = 75$  cm

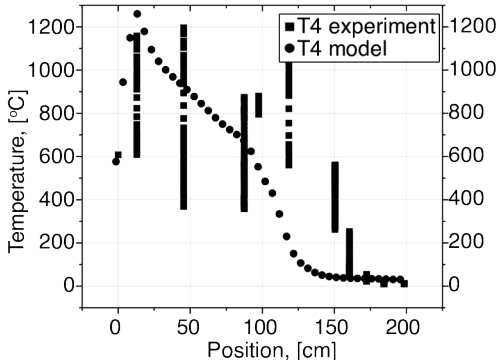


Figure 9. The temperature along the central cross-section of bale for the height  $y = 105$  cm

From the displayed images the satisfactory agreement of the measured and modelled temperature fields within bale can be observed, especially in positions  $y = 75$  cm and  $y = 45$  cm (0-30%), while in the positions  $y = 105$  cm and  $y = 15$  cm there are some higher discrepancies (10-45%) in the area of 100-125 cm from the end of combustion zone.

The temperature difference between the measured and the temperature obtained by the model varies from 0-30% in the part of the bale in the firebox (zone of higher temperature) and 10-45% in the part of the bale that has not yet entered the furnace (zone of lower temperature). A larger

difference in lower temperature area is due to the fact that the temperature level in that part is lower, and therefore the relative temperature difference (percentage) is higher.

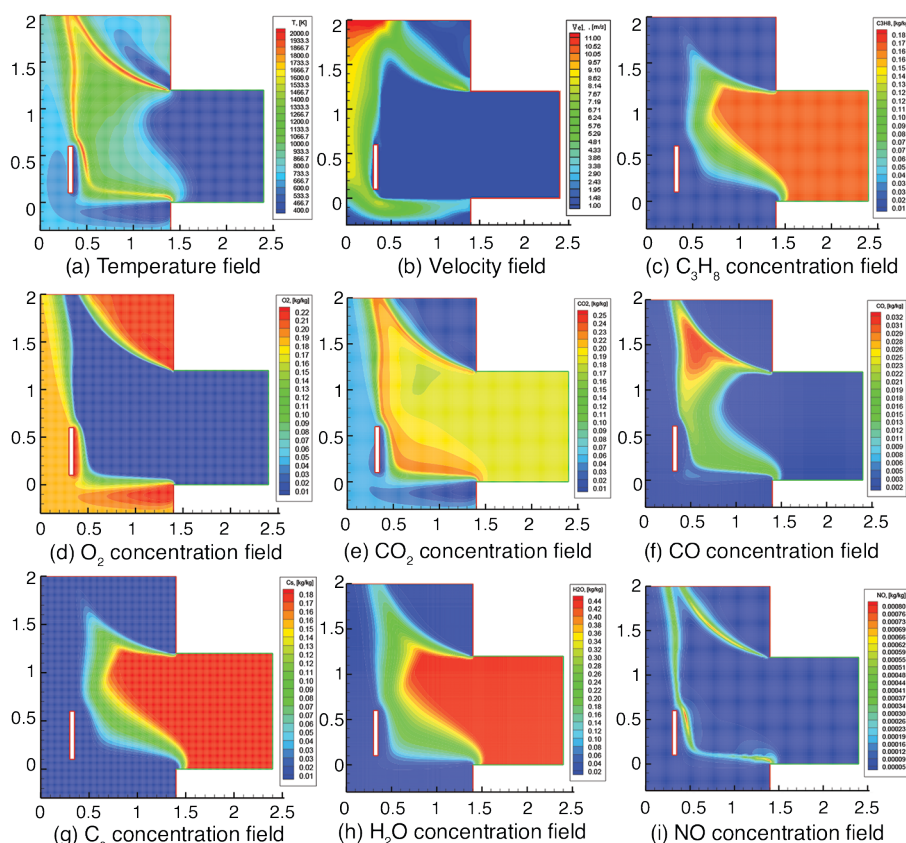
Higher temperature in the planes closest to the upper and lower surface of bales, in the positions just before entering the combustion chamber, can be explained by the bale and air input ducts are not complete seal which leads to the diffusion of oxygen, and since the temperature is high enough to create a favourable conditions for combustion. This phenomenon can be overcome by construction changes in the air supplying system.

Figure 10 shows, in addition to the simulated temperature field for which there is an experimental confirmation, and calculated fields of velocities, volatiles and flue gas components, for which there are no experimental data in this paper. However, these calculated fields are useful because from them can be drawn some conclusions in order to better understand the analyzed combustion process or to improve the combustion furnace construction, as well as to improve the proposed combustion model.

The analyses in this chapter show that the choice of the numerical simulation concept with volumetric fuel sources is justified taking account agreement with the experimental results figs. 6-9.

## Conclusion

The mathematical model of baled biomass combustion was established in such a way that simulation of combustion in stationary operating modes was enabled with sufficient



**Figure 10. Temperature, velocity and components concentration distribution obtained by numerically solving model equations (unit of measure for the axis is m).**

precision and determination of physical phenomena without unnecessary complexity, which would further extend the computational time. By the proposed model it is possible to calculate the three groups of fields: speed, temperature and components of combustion reaction (chemical species). Velocity field in the analysed area is described by the set of Navier-Stokes equations with the turbulent Reynolds stress resolving using often-used standard  $k-\varepsilon$  turbulence model. Fluid-flow in porous environment also has been described by the set of Navier-Stokes equations modified taking into account the specifics of porous media.

Model results show satisfactory agreement with experimental results both in terms of the calculated temperature and the composition of gases at the outlet cross section and in terms of temperature profiles in the central plane of soybean residue bales that participates in the combustion process. It follows that the developed two-dimensional model can be successfully used to simulate a series of the furnace working regimes, as well as to simulate the combustion of various biomasses in baled form.

### Acknowledgement

The authors thank the Ministry of Education, Science and Technological Development of Serbia for enabling funding of the projects III 42011 *Development and improvement of technologies for energy efficient and environmentally sound use of several types of agricultural and forest biomass and possible utilization for cogeneration*, TR33042 *Fluidized bed combustion*

*facility improvements as a step forward in developing energy efficient and environmentally sound waste combustion technology in fluidized bed combustors.*

### Nomenclature

|  |   |
|--|---|
| $a$ – emissivity weight factor, [–]                                    | $W$ – velocity, [ms <sup>-1</sup> ]                                   |
| $c_p$ – specific heat capacity, [kJkg <sup>-1</sup> K <sup>-1</sup> ]  | $x$ – co-ordinate, [m]  |
| $D$ – diffusivity, [m <sup>2</sup> s <sup>-1</sup> ]                   | $Y$ – mass fraction, [–]  |
| $G$ – intensity of incoming radiation, [Wm <sup>-3</sup> ]             | <i>Greek symbols</i>  |
| $H$ – specific enthalpy for creation, [Jkg <sup>-1</sup> ]             | $\Gamma$ – diffusion coefficient, [–]                                 |
| $K_1$ – viscous permeability, [m <sup>2</sup> ]                        | $\varepsilon$ – porosity, [–]   |
| $K_2$ – inertial permeability, [m]                                     | $\epsilon_r$ – emissivity, [–]  |
| $n$ – characteristic dimension, [m]                                    | $\lambda$ – thermal conductivity, [Wm <sup>-1</sup> K <sup>-1</sup> ] |
| $p$ – pressure, [Pa]   | $\mu$ – dynamic viscosity, [Pa·s]                                     |
| $R$ – components conversion rate, [kgm <sup>-3</sup> s <sup>-1</sup> ] | $\nu$ – stoichiometric number of moles, [–]                           |
| $s$ – distance, [m]  | $\rho$ – density, [kgm <sup>-3</sup> ]                                |
| $S$ – source, [kgm <sup>-3</sup> s <sup>-1</sup> ]                     | $\sigma_m$ – Schmidt number, [–]                                      |
| $T$ – temperature, [K]   |   |

### References

- [1] Miltner M., et al., 2007, Process Simulation and CFD Calculations for the Development of an Innovative Baled Biomass-Fired Combustion Chamber, *Applied Thermal Engineering*, 27 (2007), 7, pp.1138-1143
- [2] Bech, N., et al., 1996, Mathematical Modeling of Straw Bale Combustion in Cigar Burners, *Energy & Fuels*, 10 (1996), 2, pp. 276-283
- [3] Mladenović R., et al., 2008, Energy Production Facilities of Original Concept for Combustion of Soya Straw Bales, *Proceedings*, 16<sup>th</sup> European Biomass Conference & Exhibition - From Research to Industry and Markets, Valencia, Spain
- [4] Erić, A., Thermomechanical Processes Connected to Baled Soybean Residue Combustion in the Pushing Furnace, Ph. D. theses (in Serbian), Mechanical Engineering Faculty, Belgrade, 2010
- [5] Eric, A., et al., Experimental Method for Determining Forchheimer Equation Coefficients Related to Flow of Air Through the Bales of Soy Straw, *International Journal of Heat and Mass Transfer*, 54 (2011), 19-20, pp. 4300-4306
- [6] Erić, A., et al., Determination of the Stagnant Thermal Conductivity of the Baled Soybean Residue, an Original Work (in Serbian), *Contemporary Agricultural Engineering*, 36 (2010), 4, pp. 334-343
- [7] Nemoda, S., et al., Numerical Simulation of Reacting Fluid Flow in Porous Media Applied on The Biomass Combustion Research, *Proceedings*, International Conference on Computational Mechanics, (CM'04), Belgrade, 2004
- [8] Pedras, M. H. J., de Lemos, M. J. S., Thermal Dispersion in Porous Media as a Function of the Solid-Fluid Conductivity Ratio, *International Journal of Heat and Mass Transfer*, 51 (2008), 21-22, pp. 5359-5367
- [9] de Lemos, M. J. S., *Turbulence in Porous Media, Modeling and Applications*, Instituto Tecnológico de Aeronautica, San Jose dos Campos, Brasil
- [10] Kaviany, M., *Principles of Heat Transfer in Porous Media*, 2<sup>nd</sup> ed., Springer, New York, USA, 1991
- [11] Nield, D. A. , Bejan, A., *Convection in Porous Media*, Springer Science Business Media, Inc. New York, USA, 2006
- [12] Patankar, S.V., *Numerical Heat Transfer and Fluid Flow*, Hemisphere, New York, USA, 1980
- [13] Rowe, P. N., Partridge, B. A., An X-Ray Study of Bubbles in Fluidized Beds, *Trans. Inst. Chem. Eng.*, 43, (1965), pp.157-190
- [14] Davis, R. M., Taylor, G. I., The Mechanics of Large Bubbles Rising Through Extended Liquids in Tubes, *Proc. Roy. Soc.*, 200, 1950, pp.375-383